Journal of Engineering and Technology for Industrial Applications

ISSN ONLINE: 2447-0228

ITEGAM-JETIA

Manaus, v.11 n.54, p. 120-130. July/August., 2025.
DOI: https://doi.org/10.5935/jetia. v11i54.1775

RESEARCH ARTICLE OPEN ACCESS

PARAMETRIC OPTIMIZATION OF FRICTION TORQUE AND BEARING TEMPERATURE IN TAPERED ROLLER BEARINGS USING RESPONSE SURFACE METHODOLOGY

Amisha B. Khant[1], Jaydeep K. Dadhaniya[2] and Hardik G. Chothani[3]

[1] Research Scholar, Mechanical Engineering Department, Gujarat Technological University, Ahmedabad, Ahmedabad-382424 Gujarat, India.
[2] Mechanical Engineering Department, Government Engineering College Rajkot, Rajkot-360005, Gujarat, India.
[3] Mechanical Engineering Department, Government Engineering College Bhavnagar, Bhavnagar-364002, Gujarat, India

[1]https://orcid.org/0009-0002-3520-1761, [2]https://orcid.org/0009-0000-5024-3500, [3]https://orcid.org/0000-0003-2773-4365,

Email: amisha.khant@gmail.com, jaydeepdadhaniya@gmail.com, chothanihardik@yahoo.com,

ARTICLE INFO

Article History
Received: March 26, 2025
Revised: April 20, 2025
Accepted: June 15, 2025
Published: July 31, 2025

Keywords:
Analysis of Variance,
Friction Torque,
Parametric Optimization,
Response Surface Methodology,
Tapered Roller Bearings

ABSTRACT

Friction torque at high axial load increase rapidly which also raise the bearing temperature in tapered roller bearings (TRBs) that leads to major power loss and heat generation within bearing and ultimately lower bearing performance. In TRBs, at high axial load, inner raceway rib convexity plays an important role by providing resistance to friction and support the bearing. In present study, parametric optimization of friction torque and bearing temperature of TRBs are carried out using Response Surface Methodology (RSM). The RSM Box-Behnken design was used to design experiments and regression model is developed to establish the relation between input parameters inner race rib convexity, axial load and bearing shaft speed accurately. The minimum friction torque and bearing temperature are achieved at 7.96 Nm and 54.57 °C respectively at rib convexity 3.21 µ, axial load 2000 kgf and 400 bearing shaft rpm.

I. INTRODUCTION

Tapered Roller bearings (TRBs) are extensively used in aerospace, automotive, and manufacturing. These bearings are deliberated to provide high precision, reduced friction and enhanced stability against high load and speed that make them vital components in modern machinery and equipments [1–4] . Friction torque (FT) is a key parameter in TRBs as it directly influences bearing performance and plays a significant role in the operational characteristics. It affects both energy consumption and the rise in bearing temperature (BT) [5]. Accurate predicting friction torque become more important as it permit designer to calculating friction power loss and heat generation in bearing [6]. Friction torque in TRBs affected by many parameters, among all it mainly generates due to rolling between rollers & raceways and sliding frictions among roller larger ends & inner raceway rib. On the other hand the friction between cage & rollers and viscous drag are small as compared to rolling and sliding and can be neglected [7–9]. Many researchers have developed theoretical model to verify the friction torque with experimental data under different parameters.

Witte established an equation that able to predict the bearing operating torque under pure thrust, pure radial and combined trust and radial loads [10], [11]. Zhou et al. presented analytical torque model for TRBs and found good compliance with measured torques with torque test rig which runs with different lubricants and operating conditions such as two different oil, load and speed[8]. Bercea et al. suggested an analytical model to identify torque power loss in TRBs. This study presented that the power loss in the inner ring is more than the outer ring [12]. Matsuyama developed simplified formula for predicting friction torque at roller raceways due to viscous resistance for TRBs, subsequently verified with the experimental testing for the pure frictional torque for inner raceway rib. This study was later on extended for the fully flooded condition across a broad range of operating conditions for TRBs [13], [14]. Houpert compared the ball bearing torque with the TRBs for best selection according to the bearing application [15]. Black et al. evaluated rapid unique comparison method to measure running frictional torque TRBs with bearing of similar function [16]. Tiago et al. reported accurate monitoring method to measure friction torque and bearing temperature of TRBs up to 7000 N axial load and 6000 rpm rotational speed. Inner raceway rib is an important feature of the TRBs that resist the friction and support the bearing specially under high axial load [17]. M. Zander et al. presented wide comparison for calculation method results for friction in roller bearings and shows

that the contact based methods have many possibilities to predict friction accurately [18]. Karna derived an analytical expression to estimate the friction torque and found good agreement with the experimental work that carried out on newly developed test rig with detached rib under axial load up to 4000 pounds and 1600 rpm [19]. Jamison et al. observed that the contact between rib and roller is crucial to carry axial load and control bearing screwing further illustrated that maintaining adequate lubrication and accurate geometry can improve performance of the TRBs [20]. Witte and Harold quantifies friction torque sources in TRBs focusing on contact between rib and roller performance. Study explores the different operating conditions with input shaft speed 2400 rpm and apply bearing preload to input , output and axle shaft with 0.051 mm, 0.051 mm and 0.101 mm respectively along with rib and roller contact geometry and resulting friction torque [11]. Ahira et al. formulated revised equation to calculate the friction torque based on experimental data and theoretical calculation with external load up to 20 KN and speed 5000 rpm using EHL conditions for approximately 200 TRBs from bore size 17 mm to 200 mm [7]. Matsuyama et al. obtained simple formula for viscous rolling frictional torque in roller raceway contacts in TRBs using speed, material, load etc dimensionless parameters with rotational speed up to 3000 rpm and axial load upto 4 Kn [14]. T Cousseau et al. described experimental method to measure friction torque and bearing temperature for rolling bearing for axial load and rotational speed 7000N and 6000 rpm respectively using four ball Machine [17]. Y Liu et al. developed a model to analyze the effect of defects for friction torque on roller – raceways under varying loads, speed and operating temperature in TRBs using non linear spring model to statics model [21]. S Wirsching et al. identified that EHL based roller face and rib contact plays significant role for bearing power loss and presented numerical optimization technique using evolutionary algorithm for geometric parameters based on sampled DOE [22]. L Liu et al. reported new friction torque calculation model to identified the effect of raceway convexities in TRBs. Here the model is found considering inner and outer raceway surface roughness and convexity under the condition of EHL [23]. P. L. Wu et al. presented a detailed review on measurements of friction torque for different rolling bearings with explaining theoretical calculation models and experiments setups [24]. I. M.

Klebanov et al. elaborated a model to calculate wear rate due to friction torque between rib and roller contact considering spherical shape of roller end and three different shape of ribs like conical, convex and concave considered [25]. M. Manjunath et al. evaluated that at lower speed friction torque due to sliding friction between roller end and rib becomes superior when subjected to axial load with varying speeds and oil temperatures. Study presented cause of rolling resistance and thermal shear factor in TRBs by various experiments using a modular test setup[9]. P. Wingertszahn et al. identified that the friction torque between rollers end and inner raceway rib and also roller cage pockets are significant. The study suggested Parametric Multibody Simulation (PMS) model which is capable to predict friction torque and its kinematics in TRBs and validate by conducting large number of experiments [26]. S Lee et al. investigated TRBs friction torque considering roller geometries along with material uncertainties under axial load. Experimental results compared with the theoretical calculations and correlation analysis suggests that rib angle and half angle of outer raceway had considerable effect on friction torque [27]. X. Zhou et al. marked that maximum temperature in the DTRB arise between the roller end and the inner raceway rib owing to frictional heat among rollers and raceway and sliding friction between roller end and inner raceway rib specially at high axial load. The tests under pure axial load were conducted considering axial load up to 6 kN and shaft speed from 500 to 4000 rpm [28]. However previous study have identified friction torque within TRBs considering various approaches and verified these by experiments, no one have particularly addressed the effect of high pure axial load, bearing shaft speed and inner raceway rib convexity a geometrical parameter on friction torque in TRBs. These parameters are particularly became vital for those TRBs which are assembled in the heavy-duty vehicles' wheel hub and effects considerably when vehicles turn [29]. When the vehicles with heavy load are in turn, the vehicles' front wheel hub bearings experiences a high axial load and that cause rapid friction torque between the roller larger end and the rib and leads high bearing temperature. To enhance the TRBs life and reduce power loss in such conditions it is important to reduce the friction torque and manage bearing temperature by precisely estimating the effects of baring load, shaft speed, and rib convexity.

II. EXPERIMENTAL PROCEDURE

The experimental setup used in the present study is shown in Figure 1. It consists of five main units: (1) a drive unit, powered by an AC induction motor, which runs the bearing shaft at speeds of up to 1200 rpm; (2) a grease-lubricated bearing test unit, also called the bearing hub, which contains the test bearing along with a support bearing; (3) a coupling unit, which connects the drive unit to the bearing hub using two couplings and a torque sensor with a measuring capacity of up to 500 Nm; (4) a hydraulic load unit, which consists of a hydraulic cylinder controlled by an adjustable hydraulic flow control valve to vary the axial load on the test bearing up to 10,000 kgf; and (5) a SCADA (Supervisory Control and Data Acquisition) control unit, which collects data measured by torque, temperature, speed, and load sensors attached to the test rig.

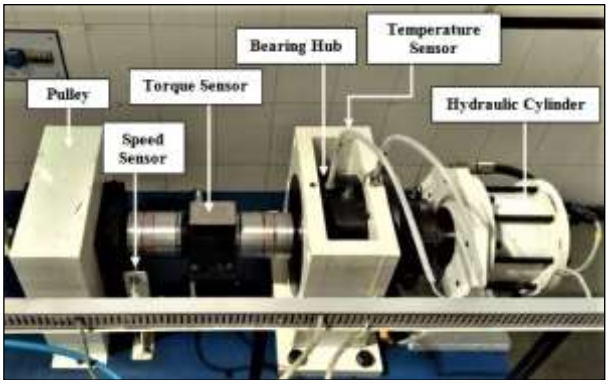

Figure 1: Experimental setup.
Source: Authors, (2024)

Three identical TRBs, with geometries as shown in Figure 2 and specifications as shown in Table 1. were selected for the experiments. These bearings had three different inner raceway rib convexities, approximately 0 µm, 3 µm, and 6 µm, measured using a TALYSURF surface roughness tester, to analyze their effect on the responses.

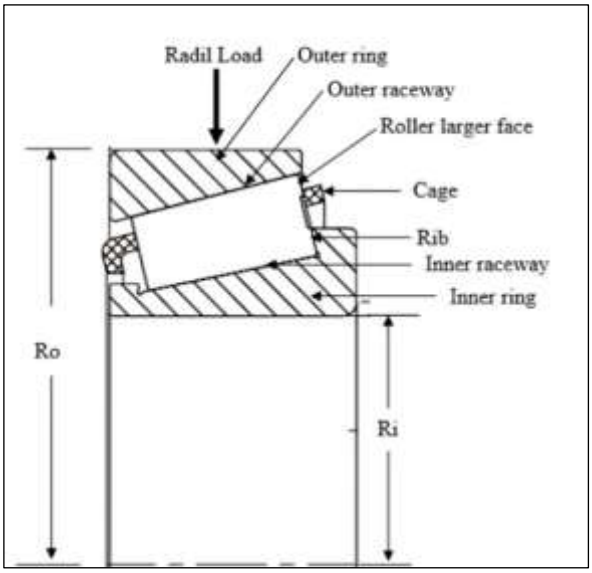

Figure 2: Tapered Roller Bearing.
Source: Authors, (2025).

Table 1: Specification of Test TRBs.

Nominal Outer diameter, mm	**150**
Nominal inner diameter, mm	90
Nominal inner ring width, mm	45
Nominal outer ring width, mm	35
Number of roller	23
Material	SAE52100

Source: Authors, (2025).

Several preliminary experiments were conducted before the final tests to determine the appropriate factor levels needed to achieve the desired objectives. During this pilot phase, the axial load was adjusted between 1,000 kgf and 8,000 kgf, the rib convexity varied from 0 to 9 µ, and the bearing speed was tested within a range of 100 to 800 rpm, in accordance with bearing specifications and intended applications. These trials explored different combinations of axial load, rib convexity, and bearing speed. Friction torque was continuously monitored using SCADA, with the highest recorded value being used for analysis and bearing temperature was measured by bearing temperature sensor attached with the tested TRB. The results and observations from the pilot experiments indicated that when the axial load exceeded 6,000 kgf and the bearing speed exceeded 600 rpm; the bearing temperature rose rapidly above 120°C, surpassing the permissible temperature range for sealed bearings as per standard guidelines. Additionally, heat generation during the tests led to discoloration on the contact surfaces of the raceway and rib. In this study, it is important to include Hertzian contact stress obtained at the roller end and inner raceway rib as high axial loads lead to increased contact stress, which raises the bearing temperature. The Hertzian contact stress can be calculated according to the applied contact types [30], here for TRBs it is applied as point contact [11] [19]. In present study contact stresses at different rib convexities and axial load combinations calculated using MESYS AG contact stress calculation software. Results ensured that up to 6µ contact stress at any axial load does not exceed 2400 MPa and it is safe as per the standards [31]. Furthermore, it was observed that when the rib convexity exceeded 6µ, the contact stress increased beyond 4,000 MPa that exceeding the permissible limits defined by bearing standards. Based on these findings, the present study focuses on three key factors, Rib Convexity (A), Axial Load (B), and Operating Speed (C) and each evaluated at three levels. Table 2 presents design factors and their three levels with coded and actual values.

Table 2: Factors and their selected levels.

Factors	Code	Level			Unit
		-1	0	1	
Rib Convexity	A	0	3	6	µ
Axial Load	B	2000	4000	6000	kgf
Bearing Speed	C	400	500	600	rpm

Source: Authors, (2025).

III. RESPONSE SURFACE METHODOLOGY (RSM)

Design of Experiments (DOE) refers to the methods used to design and analyze experiments effectively, with a minimum number of runs, while also evaluating the effective interactions between operating parameters [32], [33]. Among various DOE methods, Factorial, Response Surface, and Taguchi are the most widely used and preferred by researchers. Response Surface Methodology

(RSM) is one of the most common DOE techniques, particularly applied in sectors such as production process development, new product design, and process multi objective optimization [34], [35]. It helps researchers conduct experiments effectively, control and analyze multiple factors simultaneously, minimize resource consumption, and structure research data for easier analysis [36]–[40]. The first step in RSM is to identify the relationship between the dependent variable (y) and the independent variables (x_i). A standard second-order RSM model can be represented by Eq. (1).

$$y = \beta_0 + \beta_1 x_1 + \beta_2 x_2 + \ldots + \beta_{12} x_1 x_2 + \beta_{13} x_1 x_3 + \ldots + \beta_{11} {x_1}^2 + \beta_{22} {x_2}^2 + \cdots \quad (1)$$

The expression contains both first-degree and second-degree terms, which refine the maximum and minimum values of the response variable. The symbols β_0, β_i, and β_{ij} represent constants. The experimental values are adjusted using the polynomial regression model, as described by the above equation, to calculate the goodness of fit [33]. Response Surface Methodology (RSM) designs are further classified into two categories: 1) Central Composite Design and 2) Box-Behnken Design. In the Box-Behnken design, three-level factors (-1, 0, 1) are typically used to fit second-order models for the response. This experimental design combines 2^k factorials with an incomplete block design, resulting in designs that are generally more effective when the number of runs is large [32][40][41][42]. The present study employs the Box-Behnken design. Table 3 presents the coded Box-Behnken design matrix along with the obtained responses.

Table 3: Box Behnken design with coded factors with responses.

Run Order	A	B	C	Friction Torque (Nm)	Bearing Temperature (°C)
1	-1	-1	0	14	72
2	1	-1	0	10	73
3	-1	1	0	17	86
4	1	1	0	12	85
5	-1	0	-1	13	74
6	1	0	-1	8	74
7	-1	0	1	16	87
8	1	0	1	13	87
9	0	-1	-1	8	55
10	0	1	-1	10	64
11	0	-1	1	11	65
12	0	1	1	15	79
13	0	0	0	12	78
14	0	0	0	12	74
15	0	0	0	12	76

Source: Authors, (2025).

IV. RESULTS AND DISCUSSION

IV.1 RESPONSE SURFACE REGRESSION (RSR) MODEL

Table 4 represents the RSR model for friction torque and bearing temperature, obtained through the RSM method using MINITAB 19. These response models signify the effect of independent variables on responses by establishing a correlation between them.

Table 4: Response surface regression model for responses.

Responses	Correlation
Friction Torque	= -12.63 - 2.292 Rib Convexity - 0.000187 Axial Load + 0.0925 speed + 0.1528 Rib Convexity*Rib Convexity - 0.000000 Axial Load*Axial Load - 0.000088 speed*speed - 0.000042 Rib Convexity*Axial Load + 0.001667 Rib Convexity*speed + 0.000002 Axial Load*speed
Bearing Temperature	= -80.6 - 5.58 Rib Convexity + 0.01194 Axial Load + 0.4763 speed + 0.9861 Rib Convexity*Rib Convexity - 0.000001 Axial Load*Axial Load - 0.000437 speed*speed - 0.000083 Rib Convexity*Axial Load - 0.00000 Rib Convexity*speed + 0.000006 Axial Load*speed

Source: Authors, (2025).

IV.2 ANALYSIS OF VARIANCE (ANOVA)

ANOVA is a robust statistical method often used in mechanical experiments where multiple factors are tested simultaneously to assess their effect on the response variable. In this study, ANOVA is applied to evaluate the influence of various independent variables—axial load, speed, and rib convexity—on the response variables, friction torque and bearing temperature, as well as to assess the adequacy of the analytical model. The model includes interaction terms up to two-way interactions to improve its predictive accuracy. The ANOVA results for both responses are shown in Table 5. These table display the degrees of freedom (DF), sum of squares (SS), and p-values.

For friction torque, the model explains 99.74% of the variation, with an adjusted R-square of 99.27% and a predicted R-square of 95.85%, indicating strong reliability and applicability to the independent variables. The p-values for factors A, B, and C are less than

0.05, indicating that they have a strong influence on friction torque. However, the interaction terms AB, AC, and BC, as well as the second-order terms BB and CC, are not significant, as their p-values are higher than 0.05, indicating their impact on friction torque is negligible.

For bearing temperature, the model has an even higher R-square of 99.21%, with an adjusted R-square of 97.79% and a predicted R-square of 96.75%, demonstrating excellent fit and predictive accuracy. Factors B and C are highly significant, as their p values are less than 0.05, and strongly influencing bearing temperature. However, the terms with p values greater than 0.05 are not significant and do not affect the response. Overall, the results show that both models are well-fitted and explain most of the variation in their respective response variables.

Table 5: Analysis of Variance

Source		Friction Torque		Bearing Temperature	
	DF	SS	P-Value	SS	P-Value
Model	9	96.1500	0.000	1161.68	0.000
Linear	3	83.2500	0.000	625.25	0.000
A	1	36.1250	0.000	0.00	1.000
B	1	15.1250	0.000	300.13	0.000
C	1	32.0000	0.000	325.13	0.000
Square	3	10.6500	0.000	529.18	0.000
A*A	1	6.9808	0.000	290.83	0.000
B*B	1	0.0577	0.332	127.44	0.000
C*C	1	2.8269	0.001	70.67	0.002
2-Way Interaction	3	2.2500	0.006	7.25	0.369
A*B	1	0.2500	0.076	1.00	0.495
A*C	1	1.0000	0.007	0.00	1.000
B*C	1	1.0000	0.007	6.25	0.125
Error	5	0.2500		9.25	
Total	14	96.4000		1170.93	
R-square		99.74%		99.21%	
R-square (adj)		99.27%		97.79%	
R-square (pred)		95.85%		96.75%	

Source: Authors, (2025).

IV.3 COMPARISON OF EXPERIMENTAL RESULTS WITH RSM MODEL

Table 6 presents a comparison of the experimental results for the response variables friction torque and bearing temperature with the predicted results from the developed RSM regression model, along with the percentage error. The results show that the maximum percentage error for friction torque and bearing temperature is 2.08% and 2.7%, respectively, which is within 5%. This indicates that both models adequately fit the experimental results. Figure 3 provides a graphical comparison, illustrating how well the model predictions align with the experimental results.

Table 6: Comparison of experimental results with RSM regression model fits along percentage errors.

Run	Experimental Results		RSM Model		Percentage Error	
	FT	BT	FT	BT	FT	BT
1	14	72	13.750	72.375	1.79	0.52
2	10	73	10.000	73.375	0.00	0.51
3	17	86	17.000	85.625	0.00	0.44
4	12	85	12.250	84.625	2.08	0.44
5	13	74	13.125	74.125	0.96	0.17
6	8	74	7.875	74.125	1.56	0.17
7	16	87	16.125	86.875	0.78	0.14
8	13	87	12.875	86.875	0.96	0.14
9	8	55	8.125	54.500	1.56	0.91
10	10	64	9.875	64.250	1.25	0.39
11	11	65	11.125	64.750	1.14	0.38
12	15	79	14.875	79.500	0.83	0.63
13	12	78	12.000	76.000	0.00	2.56
14	12	74	12.000	76.000	0.00	2.70
15	12	76	12.000	76.000	0.00	0.00

Source: Authors, (2025).

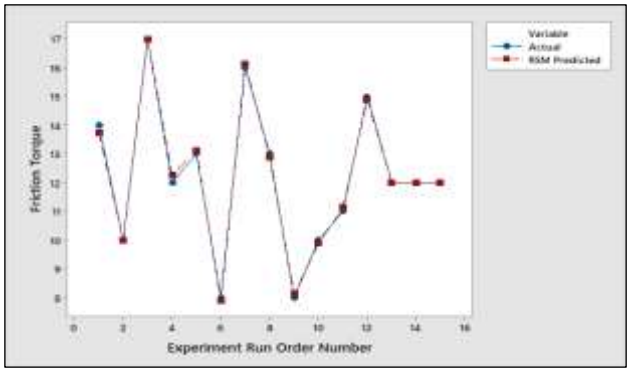

(a) Friction torque

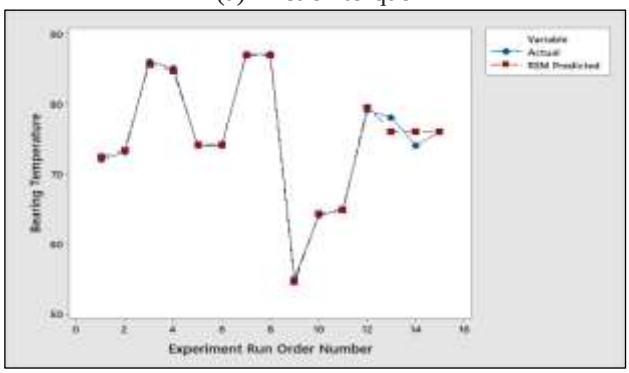

(b) Bearing Temperature

Figure 3: Experimental results vs. regression model graphs.
Source: Authors, (2025).

IV.4 INTERACTION EFFECTS BETWEEN INPUT AND OUTPUT PARAMETERS

The main effect plots for friction torque and Bearing Temperature are as shown in Figure 4 a) and b) respectively produced using MINITAB 19. It shows the effect of an independent variable on responses. Figure 4 shows that friction torque and bearing temperature increases as the axial load and bearing shaft speed increases. However, friction torque minimized at 6µ convexity while bearing temperature minimized at 3µ convexity because of contact stress between the rib and roller ends.

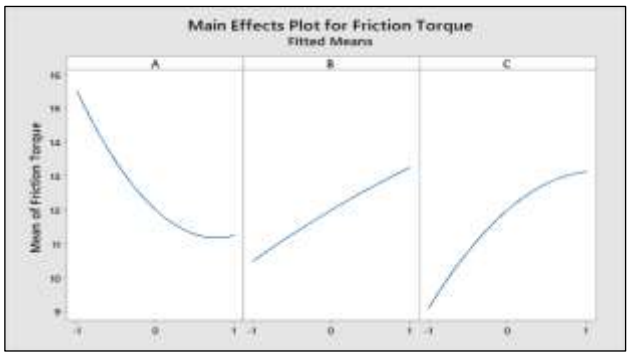

(a) Friction Torque

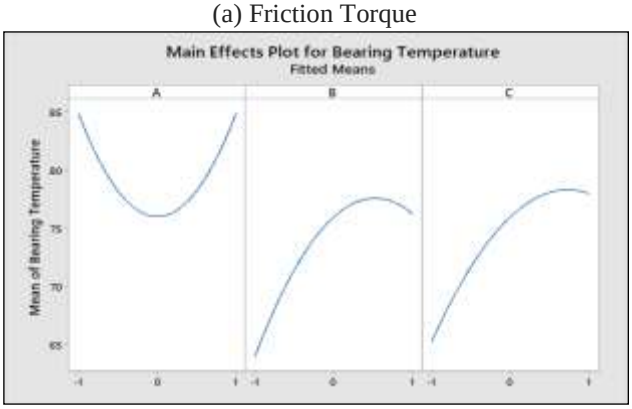

(b) Bearing Temperature.

Figure 4: Main Effect Plots.
Source: Authors, (2025).

To analyze the interaction effect of rib convexity, axial load, and bearing shaft speed on the response variables friction torque and bearing temperature, contour plots and surface plots are presented in Figure 5 and Figure 6. Figure 5(a) and (b) show the contour plots for friction torque, indicating that friction torque increases as axial load increases from 2000 kgf to 6000 kgf and speed increases from 400 rpm to 600 rpm, while it decreases as rib convexity increases from 0 µm to 6 µm. The dark-colored regions indicate higher friction torque, whereas the lightest green shade represents friction torque values below 10 Nm. Figure 5 (c) and (d) present the contour plots for bearing temperature. These plots show that bearing temperature remains minimal at 3 µm rib convexity and increases with an increase in axial load and speed.

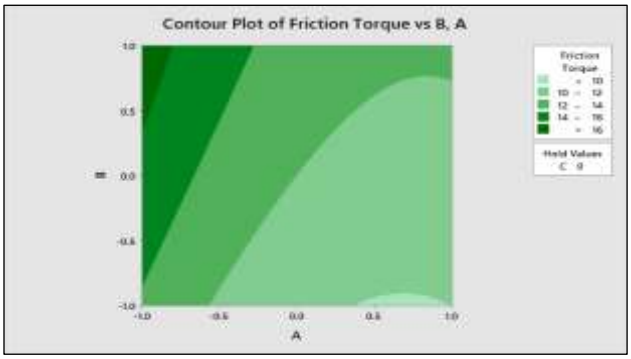

(a)

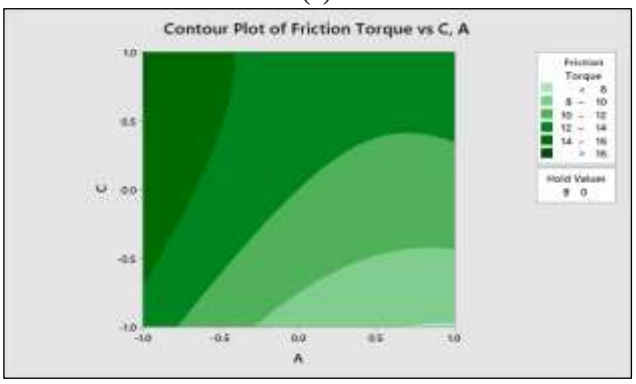

(b)

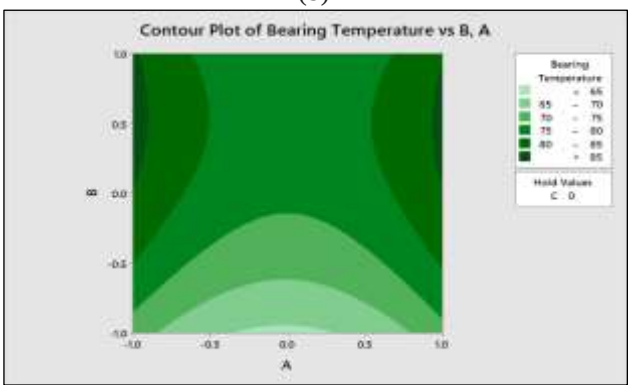

(c)

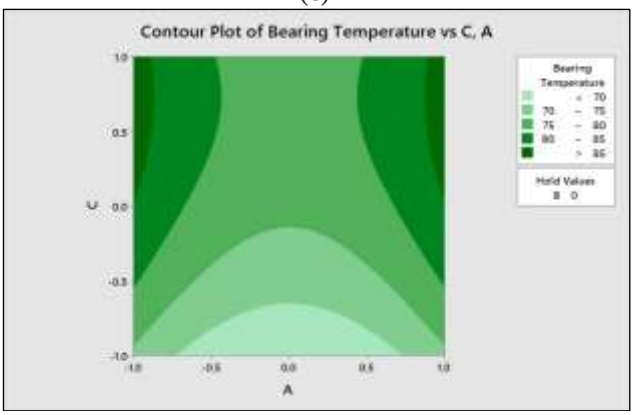

(d)

Figure 5: Contour Plots.
Source: Authors, (2025).

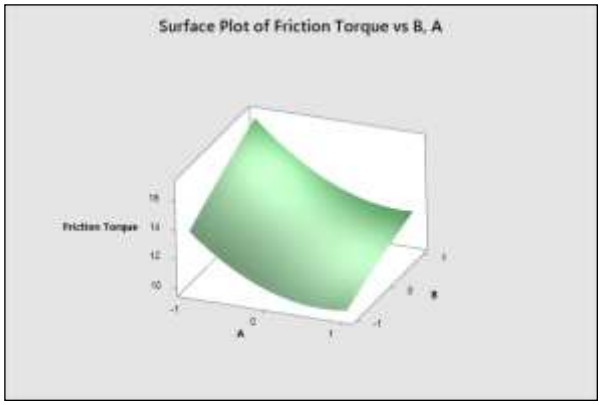

(a)

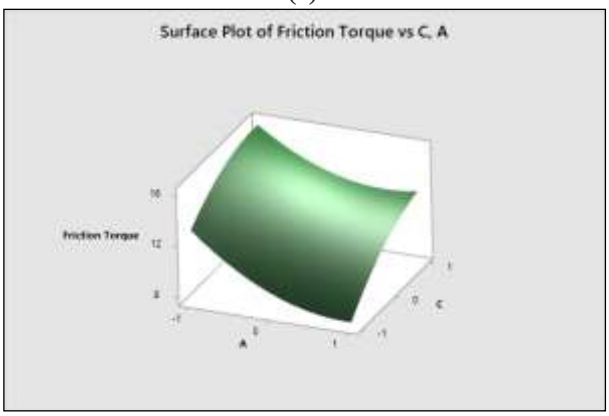

(b)

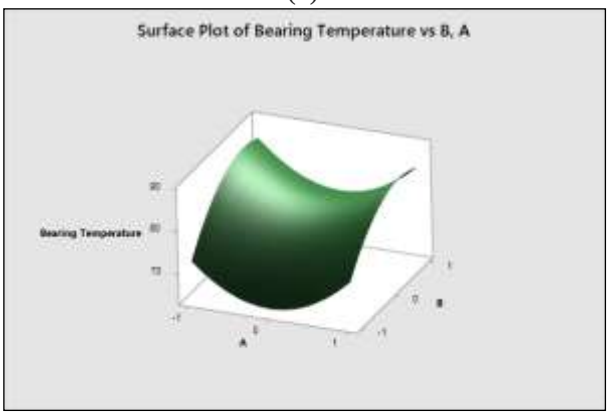

(c)

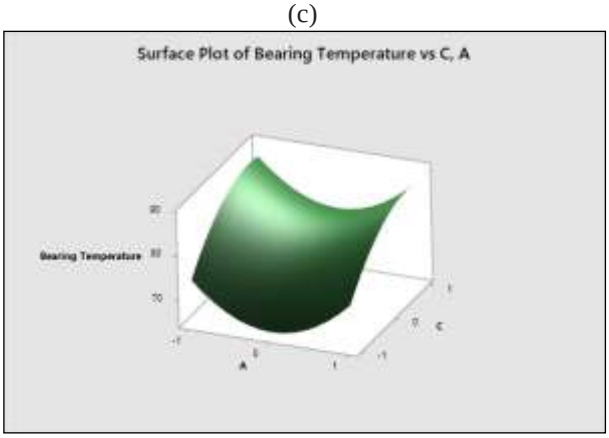

(d)

Figure 6: Surface Plots.
Source: Authors, (2025).

To visualize and analyze the effects of independent factors on response variables, Figure 6 presents the surface plots. These plots help identify maximum and minimum response values and determine the optimal combination of factor levels for optimization. Figure 6 (a) and (b) show the surface plots for friction torque, which tends to increase when rib convexity is at 0 µm, with axial load increasing from 2000 kgf to 6000 kgf and speed up to 600 rpm. However, friction torque can be minimized with an appropriate combination of rib

convexity and axial load, as shown in the figure. Similarly, Figure 6 (c) and (d) illustrate that bearing temperature remains minimal when rib convexity is set at 3 µm, with speed maintained at 400 rpm.

IV.3 PARAMETRIC OPTIMIZATION AND CONFIRMATION OF EXPERIMENTS

According to the RSM analysis results shown in Figure 7, the optimal response solutions for friction torque and bearing temperature are obtained when the parameter combination is 3.2 µm rib convexity, 2000 kgf axial load, and 400 rpm bearing shaft speed. Under these conditions, the predicted friction torque and bearing temperature are 7.96 Nm and 54.57 °C, respectively. To ensure a comprehensive analysis, two additional optimal parameter combinations obtained from the RSM were included, and confirmation experiments were conducted for these groups. Table 7 presents a comparison between the predicted and experimental results, along with the percentage deviation for all groups, which remains within 5%. Therefore, it can be concluded that the proposed statistical model accurately predicts the output responses.

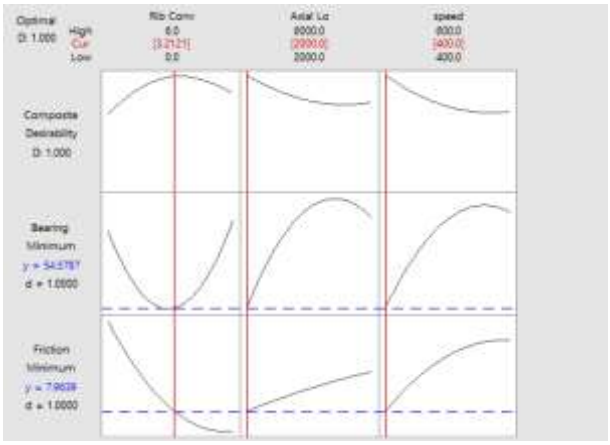

Figure 7: RSM Optimum solution.
Source: Authors, (2025).

Table 7: Optimal parameters combinations under RSM and the Deviation.

RSM Optimum Solutions	A (µ)	B (kgf)	C (rpm)		FT (Nm)	BT (° C)
1	3.2	2000	400	Predicted	7.96	54.57
				Experimental	8	56
				Deviation %	0.45	2.54
2	4.3	6000	400	Predicted	8.86	65.84
				Experimental	9	68
				Deviation %	1.60	3.18
3	0.6	2000	400	Predicted	10.82	59.53
				Experimental	11	62
				Deviation %	1.64	3.99

Source: Authors, (2025).

V. CONCLUSIONS

The present experimental study investigates the impact of operating parameters, such as high axial load and bearing speed, along with the geometrical parameter—inner race rib convexity—on friction torque and bearing temperature in tapered roller bearings (TRBs). Additionally, response surface methodology (RSM) serves as an effective statistical tool to identify the effects of these parameters on responses and optimize them for the best outcomes, ultimately minimizing overall power loss and heat generation in TRBs. According to the RSM regression model, the optimal parametric combination was found at a rib convexity of 3.21 µm, an axial load of 2000 kgf, and a bearing speed of 400 rpm, which predicted optimal responses of 7.96 Nm friction torque and 54.57 °C bearing temperature. These predicted results, along with two additional parametric combinations, were validated through confirmation tests, showing deviations within 5%. This confirms that the developed model aligns well with the experimental results and is appropriate for accurate predictions.

VI. AUTHOR'S CONTRIBUTION

Conceptualization: Amisha B. Khant, Jaydeep K. Dadhaniya and Hardik G. Chothani.
Methodology: Amisha B. Khant, Jaydeep K. Dadhaniya and Hardik G. Chothani.
Investigation: Amisha B. Khant, Jaydeep K. Dadhaniya and Hardik G. Chothani.
Discussion of results: Amisha B. Khant, Jaydeep K. Dadhaniya and Hardik G. Chothani.
Writing – Original Draft: Amisha B. Khant, Jaydeep K. Dadhaniya and Hardik G. Chothani.
Writing – Review and Editing: Amisha B. Khant, Jaydeep K. Dadhaniya and Hardik G. Chothani.
Supervision: Amisha B. Khant, Jaydeep K. Dadhaniya and Hardik G. Chothani.
Approval of the final text: Amisha B. Khant, Jaydeep K. Dadhaniya and Hardik G. Chothani.

VIII. REFERENCES

[1] T. A. Harris and M. N. Kotzalas, Essential Concepts of Bearing Technology. 2006.

[2] T. A. Harris and M. N. Kotzalas, Advanced Concepts of Bearing Technology. Taylor & Francis Group, LLC, 2006.

[3] T. A. Harris, “Rolling Bearing Analysis,” CRC Press. New York, p. pp 147–154, 2001.

[4] T. N. Wang, H. T. Li, and J. X. et al Wei, “Evaluating Stress Impact on Roller Bearing Within Disc Cutters of Tunnel Boring Machines,” Strength Mater., vol. 56, pp. 1179–1192, 2025.

[5] Palmgren A, “Ball and roller bearing engineering,” Burbank, Philadephia, p. pp 30–39, 1959.

[6] H. G. Chothani, D. J. Marsonia, N. N. Jadeda, and S. H. Zala, “LUBRICATED WORM GEARBOX ON CHURNING POWER LOSSES,” J. Eng. Technol. Ind. Appl., vol. 10, no. 49, pp. 137–143, 2024, doi: DOI: https://doi.org/10.5935/jetia.v10i49.1123.

[7] S. Aihara, “A New Running Torque Formula for TRB under axial load,” J. Tribol. ASME, vol. 109, 1987.

[8] R. S. Zhou and M. R. Hoeprich, “Torque of Tapered Roller Bearings,” J. Tribol. ASME, 1991, [Online]. Available: http://asme.org/terms

[9] M. Manjunath, D. Fauconnier, and W. Ost, “Experimental Analysis of Rolling Torque and Thermal Inlet Shear Heating in Tapered Roller Bearings,” Machines, vol. 11, 801, pp. 1–22, 2023.

[10] D. C. Witte, “Operating torque of tapered roller bearings,” ASLE Trans., vol. 16, no. 1, pp. 61–67, 1973, doi: 10.1080/05698197308982705.

[11] D. C. Witte and H. E. Hill, “Tapered roller bearing torque characteristics with emphasis on rib-roller end contact,” SAE Tech. Pap., 1987, doi: 10.4271/871984.

[12] I. Bercea, N. Mitu, I. Damian, M. Mercea, and S. Cretu, “A theoretical and experimental study on friction losses in tapered roller bearing,” Tribol. Ind., vol. 18, no. No 1, 1996.

[13] H. Matsuyama, S. Kamamoto, and K. Asano, “The analysis of frictional torque for tapered roller bearings using EHD theory,” SAE Tech. Pap., no. 724, 1998, doi: 10.4271/982029.

[14] H. Matsuyama and S. Kamamoto, “Analysis of Frictional Torque in Raceway Contacts of Tapered Roller Bearings,” KOYO Eng. J. English Ed., vol. 159, no. 159E, pp. 53–60, 2001.

[15] L. Houpert, “Ball bearing and tapered roller bearing torque: analytical, numerical and experimental results,” Tribol. Trans., vol. 45, no. 3, pp. 345–353, 2002, doi: 10.1080/10402000208982559.

[16] J. J. Blake and C. E. Truman, “Measurement of running torque of tapered roller bearings,” Proc. Inst. Mech. Eng. Part J J. Eng. Tribol., vol. 218, no. 4, pp. 239–249, 2004, doi: 10.1243/1350650041762659.

[17] T. Cousseau, B. Graça, A. Campos, and J. Seabra, “Experimental measuring procedure for the friction torque in rolling bearings,” Lubr. Sci., vol. 22, no. 4, pp. 133–147, Apr. 2010, doi: 10.1002/ls.115.

[18] M. Zander, M. Otto, T. Lohner, and K. Stahl, “Evaluation of friction calculation methods for rolling bearings,” Forsch. im Ingenieurwes. Springer, vol. 87, no. 4, pp. 1307–1316, Dec. 2023, doi: 10.1007/s10010-023-00715-1.

[19] C. L. Karna, “Performance characteristics at the rib roller end contact in tapered roller bearings,” ASLE Trans., vol. 17, no. 1, pp. 14–21, 1974, doi: 10.1080/05698197408981434.

[20] W. E. Jamison, J. J. Kauzlarich, and E. V. Mochel, “Geometric effects on the rib-roller contact in tapered roller bearings,” ASLE Trans., vol. 20, no. 1, pp. 79–88, 1977, doi: 10.1080/05698197708982820.

[21] Y. Liu, W. Kang, Y. Zhu, K. Yan, and J. Hong, “Effects of Defect on Roller-Raceway Contact State and Friction Torque of Tapered Roller Bearings,” J. Tribol., vol. 142, no. 11, Nov. 2020, doi: 10.1115/1.4047194.

[22] S. Wirsching, M. Marian, M. Bartz, T. Stahl, and S. Wartzack, “Geometrical optimization of the ehl roller face/rib contact for energy efficiency in tapered roller bearings,” Lubricants, vol. 9, no. 67, pp. 1–19, 2021, doi: 10.3390/lubricants9070067.

[23] L. Liu, W. Liu, K. Wang, D. Wang, and Y. Wang, “Effects of Raceway Convexity on Friction Moment of Tapered Roller Bearings,” J. Phys. Conf. Ser. Pap., 2022, doi: 10.1088/1742-6596/2174/1/012047.

[24] P. L. Wu et al., “Theoretical calculation models and measurement of friction torque for rolling bearings: state of the art,” J. Brazilian Soc. Mech. Sci. Eng., vol. 44, no. 9, 2022, doi: 10.1007/s40430-022-03726-1.

[25] I. M. Klebanov, A. M. Brazhnikova, and K. A. Polyakov, “Tapered Roller Bearing Rib-Roller End Interaction at Hydrodynamic Contact,” J. Frict. Wear, vol. 43, no. 6, pp. 391–397, 2022, doi: 10.3103/S106836662206006X.

[26] P. Wingertszahn, O. Koch, L. Maccioni, F. Concli, and B. Sauer, “Predicting Friction of Tapered Roller Bearings with Detailed Multi-Body Simulation Models,” Lubricants, vol. 11, no. 9, 2023, doi: 10.3390/lubricants11090369.

[27] S. Lee and H. G. An, “Evaluation of Friction Torque in Tapered Roller Bearings,” SAE Int., p. 6, 2024, doi: https://doi.org/10.4271/2024-01-3047.

[28] X. Zhou, Z. Ge, X. Li, M. Rao, and Q. Han, “Thermal Analysis of Grease-Lubricated Double Row Tapered Roller Bearings,” Lubricants, vol. 13(2), 2025, doi: https://doi.org/10.3390/lubricants13020084.

[29] B. Martin and H. E. Hill, “Design and selection factors for automatic transaxle tapered roller bearings,” SAE Tech. Pap., 1992, doi: 10.4271/920609.

[30] M. Gärtner et al., “Evaluation of hybrid spindle bearings with nitriding raceway steels under high rotational speeds,” Tribol. Mater., vol. 2, no. 3, pp. 88–98, 2023, doi: 10.46793/tribomat.2023.012.

[31] SKF, “SKF GENERAL CATALOGUE,” SKF: Gothenburg, Sweden, 2003. [Online]. Available: https://imparayaycia.com/SKF CATALOGO GENERAL.pdf

[32] R. A. Fisher, “The Design of Experiments.,” Hafner Press, no. 9th Edition. p. 256, 1974. doi: 10.2307/2348207.

[33] D. C. Montgomery, Design and analysis of experiments. 2013. doi: 10.2307/2983009.

[34] M. M. Muanda, P. P. D. Omalanga, V. M. Mitonga, and M. N. Ilunga, “Gold Removal From Gold-Bearing Ore Using Alpha-Cyclodextrin: Response Surface Methodology and Artificial Neural Analysis Network Optimizations,” J. Eng. Technol. Ind. Appl., vol. 9, no. 42, pp. 48–60, 2023, doi: 10.5935/jetia.v9i42.879.

[35] É. S. Passari, H. J. Amorim, and A. J. Souza, “Multiobjective Optimization of Cutting Parameters for Finishing End Milling Hardox® 450,” J. Eng. Technol. Ind. Appl., vol. 8, no. 34, pp. 20–28, 2022, doi: 10.5935/jetia.v8i34.805.

[36] A. I. Khuri and J. A. Cornell, “Response Surfaces: Designs and Analyses Second Edition (2nd ed.).,” CRC Press. Boca Rat., 1996, doi: https://doi.org/10.1201/9780203740774.

[37] E. R. Ziegel, “Response Surfaces: Designs and Analyses,” Technometrics, vol. 39, no. 3, p. 342, 1997, doi: https://doi.org/10.1080/00401706.1997.10485140.

[38] C. M. Anderson-Cook, C. M. Borror, and D. C. Montgomery, “Response surface design evaluation and comparison,” J. Stat. Plan. Inference, vol. 139, no. 2, pp. 629–641, 2009, doi: 10.1016/j.jspi.2008.04.004.

[39] A. I. Khuri and Siuli Mukhopadhyay, “Response surface methodology,” WIREs Comput. Stat., vol. 2, no. 2, pp. 128–149, 2010, doi: https://doi.org/10.1002/wics.73.

[40] A. Dean, V. D., and D. Draguljić, Response Surface Methodology. Design and Analysis of Experiments. 2017. doi: 10.1007/978-3-319-52250-0.

[41] A. Yıldız, L. Uğur, and İ. E. Parlak, “Optimization of the Cutting Parameters Affecting the Turning of AISI 52100 Bearing Steel Using the Box-Behnken Experimental Design Method,” Appl. Sci., vol. 13, no. 1, 2023, doi: 10.3390/app13010003.

[42] S. Bhivsane, A. Chel, and S. Sayyed, “Machining Parameters Optimization in Wet Turning of En31 Material Using Box-Behnken Approach of Rsm,” J. Eng. Technol. Ind. Appl., vol. 10, no. 50, pp. 103–111, 2024, doi: 10.5935/jetia.v10i50.1354.